Oxygen DX center in $In_{0.17}Al_{0.83}N$: Nonradiative recombination and persistent photoconductivity

Rocco Meli, Giacomo Miceli, and Alfredo Pasquarello
Chaire de Simulation à l'Echelle Atomique (CSEA), Ecole Polytechnique Fédérale de Lausanne (EPFL), CH-1015 Lausanne, Switzerland

(Received 16 December 2016; accepted 27 January 2017; published online 13 February 2017)

Using a hybrid density-functional scheme, we address the O impurity substitutional to N (O_N) in $In_{0.17}Al_{0.83}N$. Our modelling supports In clustering to account for the strong band-gap bowing observed in $In_xAl_{1-x}N$ alloys. To study the O_N defect in $In_{0.17}Al_{0.83}N$ alloys, we therefore consider a model containing an In cluster and find that the most stable configuration shows four In nearest neighbors. We show that such a O_N defect forms a DX center and gives rise to two defect levels at 0.70 and 0.41 eV below the conduction band edge, in good agreement with experiment. The calculated defect energetics entail a fast nonradiative recombination upon photoexcitation at room temperature and account for the observation of persistent photoconductivity at low temperature. *Published by AIP Publishing*. [http://dx.doi.org/10.1063/1.4975934]

In the last decades, $In_xAl_{1-x}N$ has attracted a great deal of interest for its possible applications in electronic and optoelectronic devices.[1–3] In particular, $In_{0.17}Al_{0.83}N$ is nearly lattice matched to GaN and can be used to realize strain-free heterostructures.[4,5] Applications include distributed Bragg reflectors, thick cladding layers in edge emitting lasers, waveguides exploiting the large difference in refractive indices between InAlN and GaN, and high-electron mobility transistors (HEMTs).[6–8]

To control the electronic properties of these materials, it is important to understand the role of impurities. Upon growth through metalorganic vapor phase epitaxy (MOVPE), it is known that considerable concentrations of oxygen and carbon impurities are incorporated.[8] Experimental investigations have identified various defect states with activation energies ranging between 200 and 500 meV.[9–11] However, their origin has been difficult to ascertain and it has remained unclear whether these states relate to point defects or to dislocations. More recently, defect states have been measured at 68 meV and 270 meV and tentatively assigned to oxygen based on their concentration.[12] The observation of persistent photoconductivity (PPC) effects has been taken as an indication supporting this interpretation,[12] as oxygen is known to give rise to deep donor levels (DX centers) in AlN.[13]

In this Letter, we study the oxygen impurity substitutional to nitrogen (O_N) in $In_{0.17}Al_{0.83}N$ through density-functional-theory calculations. We find that O_N gives defect levels that are in agreement with experimental observations. These impurities behave like DX centers and can explain the origin of the persistent photoconductivity effects.

In our calculations, we make use of the semilocal density functional introduced by Perdew, Burke, and Ernzerhof (PBE),[14] and the hybrid functional introduced by Heyd, Scuseria, and Ernzerhof (HSE).[15,16] In the latter, the fraction of Fock exchange is set to $\alpha = 0.37$ for AlN and to $\alpha = 0.19$ for InN in order to reproduce their experimental bandgaps. For intermediate $In_xAl_{1-x}N$ alloys, the mixing coefficient α is linearly interpolated. We use normconserving pseudopotentials to treat core-valence interactions and a kinetic energy cutoff of 70 Ry to expand the valence wave functions in a plane-wave basis set. The Brillouin zone is sampled with a $2 \times 2 \times 2$ Monkhorst-Pack grid of **k** points.[17] All structures are relaxed at the PBE level of theory, and the optimal lattice parameters are obtained by means of Murnaghan's equation of state.[18] Both semilocal and hybrid-functional calculations are performed using the Quantum-ESPRESSO suite of programs.[19] The HSE implementation and the treatment of the exchange potential are described in Refs. 20 and 21, respectively.

The formation energy of the O_N impurity in the charge state q is defined as

$$E_f[O_N^q] = \Delta E_{tot} + \mu_N - \mu_O + q(\epsilon_v + \epsilon_F + \Delta V_{0/b}) + E_{corr}^q, \quad (1)$$

where $\Delta E_{tot} = E_{tot}[O_N^q] - E_{tot}[\text{bulk}]$ is the total energy difference between the defective and the pristine systems, μ_N and μ_O are the chemical potentials of nitrogen and oxygen, respectively, and ϵ_F is the Fermi energy referred to the valence band maximum ϵ_v. $\Delta V_{0/b}$ is the potential alignment term between the neutral and the charged supercells. E_{corr}^q is a state-of-the-art correction term which accounts for electrostatic finite-size effects.[22,23] Thus, we apply corrections of 0.19 eV for the defects in the charge state $q = \pm 1$. Defect levels are here defined as thermodynamic charge transition levels and correspond to the values of the Fermi energy ϵ_F at which the formation energies E_f of two different charge states are equal. In this work, the O impurity is modeled with 96-atom supercells, leading to a localized state with an impurity band width lower than 0.02 eV. We here focus on relative formation energies and charge transition levels. Absolute formation energies, which would determine defect concentrations, remain out of reach as they depend on elemental chemical potentials and on the position of the Fermi level during growth, which are difficult to assess experimentally.

The defect levels in this work are first obtained at the PBE level and then positioned with respect to the HSE band

edges through an alignment procedure based on the average electrostatic potential.[24,25] This scheme preserves the overall accuracy of hybrid functional calculations,[26–30] but significantly reduces the computational cost, thereby making possible the study of a large variety of defect positions within a disordered alloy, such as $In_{0.17}Al_{0.83}N$. To illustrate the accuracy of this scheme in the case of III–V compounds, we focused on the O_N impurity in AlN. In agreement with previous studies,[13,31–33] we found that the defect is only stable in the singly positive and singly negative charge states, the latter being particularly stabilized by a displacement of the O atom out of the regular lattice site. Within our PBE-based scheme, the $+/-$ charge transition level occurs at 5.56 eV from the valence band maximum, in very close agreement with the result found at 5.57 eV within a fully HSE-based approach. The present set-up is also validated by the comparison with a previous calculation, which reports the defect level at 5.46 eV.[13]

A common method to study alloys within the supercell approximation is to use special quasirandom structures (SQSs), where the atoms are positioned within the lattice in such a way that they reproduce at best the correlation functions of a random alloy.[37] To assess the validity of this approach for $In_xAl_{1-x}N$, we generated periodic SQS models of 96 atoms with the Alloy Theoretic Automated Toolkit (ATAT) software and calculated the corresponding bandgaps.[38–43] As shown in Fig. 1, we found that SQSs systematically overestimate the experimental bandgaps with a bowing parameter of 2.93 eV, much smaller than the experimental one of about ∼6 eV.[44] We therefore considered structural models of the same size in which the In atoms are grouped together within a single cluster. This leads to a reduction of the calculated bandgaps and to a bowing parameter of 5.1 eV, in much better agreement with experiment (Fig. 1). Our results support previous theoretical studies, which proposed In clustering as the cause of the unusually strong bandgap bowing observed in $In_xAl_{1-x}N$.[45–48] In our study of the oxygen impurity, we therefore adopt a structural model, in which the In atoms are clustered. To achieve a composition of $x = 0.17$, we considered a compact cluster of 8 In

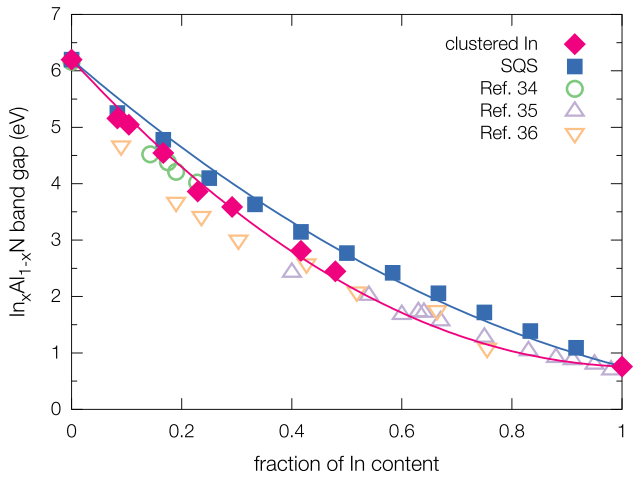

FIG. 1. Calculated bandgap of $In_xAl_{1-x}N$ as a function of the In content for SQSs and clustered In structures. The theoretical results are compared with experimental measurements.[34–36] The solid lines correspond to a quadratic fit of the calculated points.

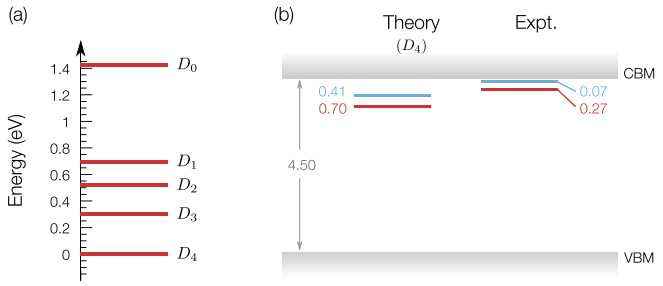

FIG. 2. (a) Formation energies of O_N impurities in $In_{0.17}Al_{0.83}N$ alloys. For a given number n of In nearest neighbors, only the most stable defects D_n are reported. The Fermi energy is taken at the conduction band (n-type conditions). (b) Calculated defect levels (in eV) of the most stable O_N defect (D_4), compared to experimental defect levels (Ref. 12). Red and blue levels refer to +/0 and 0/– charge transition levels. The defect levels are referred to the conduction band minimum (CBM).

atoms in a 96-atom supercell. We use an orthorhombic supercell to accommodate the wurzite structure of the semiconductor. For this model, we found a relaxed lattice parameter of 3.19 Å, a c/a ratio of 1.603, and a bandgap of 4.47 eV, to be compared with their experimental counterparts of 3.18 Å (Ref. 49), 1.605 (Ref. 49), and 4.5 eV (Ref. 50), respectively.

To account for the various chemical environments in the disordered alloy, we investigated all the possible sites for O_N in the adopted structural model. In particular, the considered sites differ by the In coordination, which varies between 0 and 4. To compare the stability of the oxygen impurity in the various chemical environments, we assume n-type conditions, as observed experimentally.[51,52] In these conditions, the impurity is always found in the charge state $q = -1$. As can be seen in Fig. 2, the stability of the defect increases with the number of nearest neighbor In atoms. The most stable defect state corresponds to a site with a fourfold In coordination (D_4), the next most stable state (D_3) lying higher in energy by 0.30 eV. This finding suggests that the incorporation of oxygen in an $In_xAl_{1-x}N$ alloy preferentially occurs inside the In clusters.

For all the lowest-energy sites, the defects are stable in their singly positive, neutral, and singly negative charge states. In particular, D_4 shows a symmetric tetrahedral configuration in the singly positive and in the neutral state (D_4^s), but undergoes a noticeable distortion (D_4^d) upon the trapping of one electron (cf. Fig. 3). Among the most stable defects, such a DX-like behavior is only found for the fourfold In coordination, when all the nearest neighbors belong to the

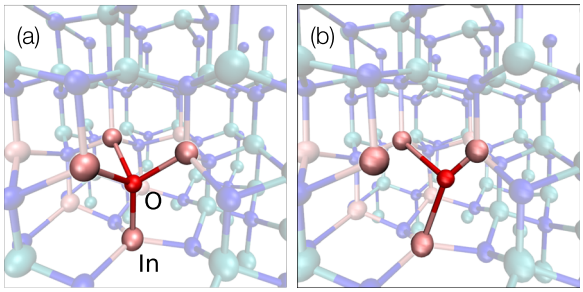

FIG. 3. The DX behavior of the most stable oxygen defect in $In_{0.17}Al_{0.83}N$: (a) a symmetric neutral state $(D_4^s)^0$ and (b) a distorted negatively charged state $(D_4^d)^-$.

same atomic species. Irrespective of the In coordination, the most stable defects always show two defect states in close proximity of the conduction band. For D_4, we calculated $+/0$ and $0/-$ charge transition levels at 0.70 and 0.41 eV below the conduction band, respectively. These defect levels are in good agreement with the energies measured at 0.27 and 0.07 eV by Py *et al.*[12] [cf. Fig. 2(b)]. In particular, the calculated separation of 0.29 eV between the localized defect levels, which is more robust than the separation from the delocalized conduction band,[24,25] also shows excellent agreement with the separation of 0.2 eV between the measured levels.[12] This level of correspondence strongly supports the assignment of the experimentally identified levels to the O_N impurity.

Next, we investigate whether the O_N DX center could be at the origin of the persistent photoconductivity effect observed at low temperature in $In_{0.17}Al_{0.83}N$. To this aim, we compare the energies of the D_4 in its neutral and negatively charged states along a configurational path connecting the symmetric D_4^s and the distorted D_4^d configurations. For the two charge states, we obtain the minimum-energy path through nudged-elastic-band calculations.[53] The path obtained in this way describes the continuous transformation from the symmetric structure of the D_4 defect [Fig. 3(a)] into its distorted structure [Fig. 3(b)]. The relative energy along the path is obtained through Eq. (1) and depends on the Fermi level ϵ_F. We remark that upon a downward shift of ϵ_F, the negatively charged state is destabilized with respect to the neutral one.

We first consider room temperature conditions. Experimental measurements report a residual *n*-type conductivity with a carrier density of $1 \times 10^{16}\,cm^{-3}$ (Refs. 51 and 52). From the charge neutrality equations for semiconductors dominated by impurities,[54,55] we inferred that ϵ_F lies at 0.16 eV below the conduction band edge. The energy profiles of the two charge states along the distortion paths are illustrated in Fig. 4(a). Our calculations suggest the following interpretation. In its ground state, the defect is in a negatively charged state with an electron trapped in the distorted $(D_4^d)^-$ configuration. Upon illumination with photon energies higher than 1.70 eV, the electron is promoted to the conduction band and the defect switches to its neutral charge state [$(D_4^d)^0$, red curve in Fig. 4]. In this charge state, the defect can relax to the symmetric $(D_4^s)^0$ configuration, recapture an electron in a nonradiative way, and return without overcoming any barrier to its distorted $(D_4^d)^-$ ground state. This mechanism is consistent with the absence of any persistent conductivity upon photoexcitation at room temperature.[12]

We put forward the following model for explaining the appearance of persistent photoconductivity at a temperature of 100 K.[12] At this temperature, we expect a reduction in the concentration of ionized donors and a consequent downshift of ϵ_F. Temperature-dependent entropic effects on the formation energies are negligible and can be neglected.[55] Hence, the variation of the Fermi energy destabilizes $(D_4^s)^-$ through a rigid upwards shift of its minimum energy path. Our calculations indicate that it is sufficient to assume a downshift of the Fermi energy lower than 0.1 eV to destabilize $(D_4^s)^-$ with respect to the $(D_4^s)^0$ [cf. separation energy in Fig. 4(a)]. This leads to an energy barrier E_b for the nonradiative recombination process from $(D_4^s)^0$ to $(D_4^d)^-$, as illustrated qualitatively

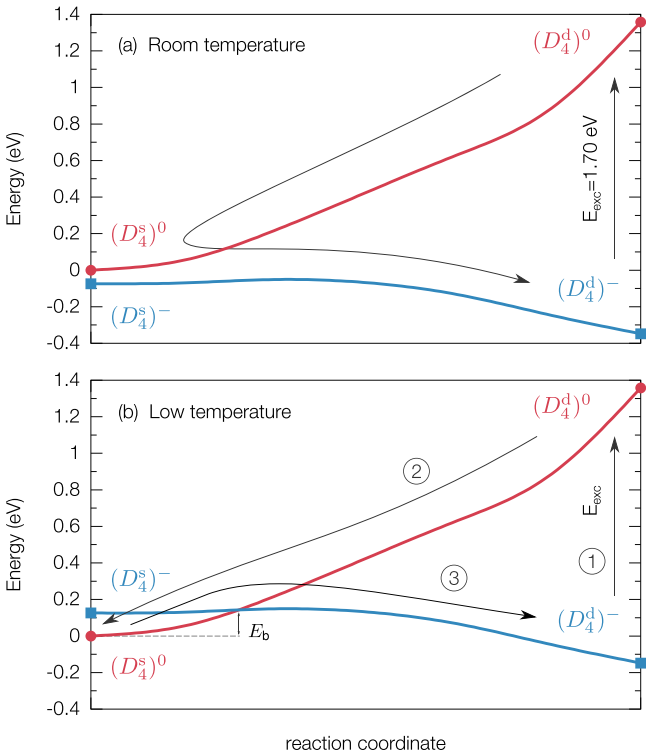

FIG. 4. Configurational diagram based on defect formation energy calculations along the path between the symmetric D_4^s and the distorted D_4^d structures of the oxygen impurity. Intermediate configurations in the neutral and negative charge states are obtained through nudged-elastic-band calculations. Panel (a) corresponds to room-temperature conditions, at which the Fermi energy is estimated to lie at 0.16 eV below the conduction band edge. Panel (b) qualitatively illustrates the lowering of the Fermi energy achieved at low temperature and the consequent creation of an energy barrier E_b for the nonradiative recombination.

in Fig. 4(b). In this model, the ground state still corresponds to the negatively charged $(D_4^d)^-$. Upon ① photoexcitation, the defect switches to the neutral charge state and ② relaxes to the symmetric $(D_4^s)^0$. The barrier E_b then prevents ③ immediate recombination, and the defect temporarily remains in the neutral metastable $(D_4^s)^0$ configuration. This configuration involves free electrons in the conduction band, which are responsible for the observed persistent photoconductivity.[12]

In conclusion, we have shown that the O_N impurity in $In_{0.17}Al_{0.83}N$ is a DX center, which accounts well for the experimental observations. The calculated energetics entail two defect levels observed in the vicinity of the conduction band edge and the appearance of persistent photoconductivity as the temperature is reduced.

We acknowledge fruitful interactions with A. Alkauskas, N. Grandjean, L. Lugani, and M. A. Py. Financial support is acknowledged from the Swiss National Science Foundation (Grant No. 200020-152799). We used computational resources of CSCS and CSEA-EPFL.

[1]S. Yamaguchi, M. Kariya, S. Nitta, H. Kato, T. Takeuchi, C. Wetzel, H. Amano, and I. Akasaki, J. Cryst. Growth **195**, 309 (1998).
[2]D. Li, X. Dong, J. Huang, X. Liu, Z. Xu, X. Wang, Z. Zhang, and Z. Wang, J. Cryst. Growth **249**, 72 (2003).
[3]D. S. Katzer, D. F. Storm, S. C. Binari, B. V. Shanabrook, A. Torabi, L. Zhou, and D. J. Smith, J. Vac. Sci. Technol. B **23**, 1204 (2005).
[4]K. Lorenz, N. Franco, E. Alves, I. M. Watson, R. W. Martin, and K. P. O'Donnell, Phys. Rev. Lett. **97**, 085501 (2006).

[5]R. Butté, J.-F. Carlin, E. Feltin, M. Gonschorek, S. Nicolay, G. Christmann, D. Simenov, A. Castiglia, J. Dorsaz, H. J. Buehlmann, S. Christopoulos, G. Baldassarri Höger von Högersthal, A. J. D. Grundy, M. Mosca, C. Pinquier, M. A. Py, F. Demangeot, J. Frandon, P. G. Lagoudakis, J. J. Baumberg, and N. Grandjean, J. Phys. D: Appl. Phys. **40**, 6328 (2007).
[6]J.-F. Carlin and M. Ilegems, Appl. Phys. Lett. **83**, 668 (2003).
[7]A. Castiglia, E. Feltin, J. Dorsaz, G. Cosendey, J.-F. Carlin, R. Butté, and N. Grandjean, Electron. Lett. **44**, 521 (2008).
[8]M. A. Py, L. Lugani, Y. Taniyasu, J.-F. Carlin, and N. Grandjean, J. Appl. Phys. **117**, 185701 (2015).
[9]D. Johnstone, J. H. Leach, V. A. Kovalskii, Q. Fan, J. Xie, and H. Morkoç, SPIE Proc. Ser. **7216**, 72161 (2009).
[10]W. Chikhaoui, J.-M. Bluet, M.-A. Poisson, N. Sarazin, C. Dua, and C. Bru-Chevallier, Appl. Phys. Lett. **96**, 072107 (2010).
[11]Z. Chen, K. Fujita, J. Ichikawa, Y. Sakai, and T. Egawa, Jpn. J. Appl. Phys. **50**, 081001 (2011).
[12]M. A. Py, L. Lugani, Y. Taniyasu, J.-F. Carlin, and N. Grandjean, Phys. Rev. B **90**, 115208 (2014).
[13]L. Gordon, J. L. Lyons, A. Janotti, and C. G. Van de Walle, Phys. Rev. B **89**, 085204 (2014).
[14]J. P. Perdew, K. Burke, and M. Ernzerhof, Phys. Rev. Lett. **77**, 3865 (1996).
[15]J. Heyd, G. E. Scuseria, and M. Ernzerhof, J. Chem. Phys. **118**, 8207 (2003).
[16]J. Heyd, G. E. Scuseria, and M. Ernzerhof, J. Chem. Phys. **124**, 219906 (2006).
[17]H. J. Monkhorst and J. D. Pack, Phys. Rev. B **13**, 5188 (1976).
[18]F. D. Murnaghan, P. Natl. Acad. Sci. U. S. A **30**, 244 (1944).
[19]P. Giannozzi, S. Baroni, N. Bonini, M. Calandra, R. Car, C. Cavazzoni, D. Ceresoli, G. L. Chiarotti, M. Cococcioni, I. Dabo, A. Dal Corso, S. de Gironcoli, S. Fabris, G. Fratesi, R. Gebauer, U. Gerstmann, C. Gougoussis, A. Kokalj, M. Lazzeri, L. Martin-Samos, N. Marzari, F. Mauri, R. Mazzarello, S. Paolini, A. Pasquarello, L. Paulatto, C. Sbraccia, S. Scandolo, G. Sclauzero, A. P. Seitsonen, A. Smogunov, P. Umari, and R. M. Wentzcovitch, J. Phys. Condens. Mat. **21**, 395502 (2009).
[20]H.-P. Komsa, P. Broqvist, and A. Pasquarello, Phys. Rev. B **81**, 205118 (2010).
[21]P. Broqvist, A. Alkauskas, and A. Pasquarello, Phys. Rev. B **80**, 085114 (2009).
[22]C. Freysoldt, J. Neugebauer, and C. G. Van de Walle, Phys. Rev. Lett. **102**, 016402 (2009).
[23]H.-P. Komsa, T. T. Rantala, and A. Pasquarello, Phys. Rev. B **86**, 045112 (2012).
[24]A. Alkauskas, P. Broqvist, and A. Pasquarello, Phys. Rev. Lett. **101**, 046405 (2008).
[25]A. Alkauskas, P. Broqvist, and A. Pasquarello, Phys. Status Solidi B **248**, 775 (2011).
[26]A. Alkauskas and A. Pasquarello, Phys. Rev. B **84**, 125206 (2011).
[27]G. Miceli and A. Pasquarello, Microelectron. Eng. **109**, 60 (2013).
[28]G. Miceli and A. Pasquarello, Microelectron. Eng. **147**, 51 (2015).
[29]D. Colleoni, G. Miceli, and A. Pasquarello, Phys. Rev. B **92**, 125304 (2015).
[30]D. Colleoni, G. Miceli, and A. Pasquarello, Microelectron. Eng. **147**, 260 (2015).
[31]T. Mattila and R. M. Nieminen, Phys. Rev. B **54**, 16676 (1996).
[32]C. H. Park and D. J. Chadi, Phys. Rev. B **55**, 12995 (1997).
[33]L. Silvestri, K. Dunn, S. Prawner, and F. Ladouceur, Appl. Phys. Lett. **99**, 122109 (2011).
[34]E. Sakalauskas, H. Behmenburg, C. Hums, P. Schley, G. Rossbach, C. Giesen, M. Heuken, H. Kalisch, R. H. Jansen, J. Bläsing, A. Dadgar, A. Krost, and R. Goldhahn, J. Phys. D: Appl. Phys. **43**, 365102 (2010).
[35]R. E. Jones, R. Broesler, K. M. Yu, J. W. Ager III, E. E. Haller, W. Walukiewicz, X. Chen, and W. J. Schaff, J. Appl. Phys. **104**, 123501 (2008).
[36]E. Iliopoulos, A. Adikimenakis, C. Giesen, M. Heuken, and A. Georgakilas, Appl. Phys. Lett. **92**, 191907 (2008).
[37]A. Zunger, S.-H. Wei, L. G. Ferreira, and J. E. Bernard, Phys. Rev. Lett. **65**, 353 (1990).
[38]A. van de Walle and G. Ceder, J. Phase Equilib. **23**, 384 (2002).
[39]A. van de Walle and M. Asta, Modell. Simul. Mater. Sci. Eng. **10**, 521 (2002).
[40]A. van de Walle, M. Asta, and G. Ceder, CALPHAD **26**, 539 (2002).
[41]G. L. W. Hart and R. W. Forcade, Phys. Rev. B **77**, 224115 (2008).
[42]A. van de Walle, CALPHAD: Comput. Coupling Phase Diagrams Thermochem. **33**, 266 (2009).
[43]A. van de Walle, P. Tiwary, M. M. de Jong, D. L. Olmsted, M. D. Asta, A. Dick, D. Shin, Y. Wang, L.-Q. Chen, and Z.-K. Liu, CALPHAD: Comput. Coupling Phase Diagrams Thermochem. **42**, 13 (2013).
[44]K. Wang, R. W. Martin, D. Amabile, P. R. Edwards, S. Hernandez, E. Nogales, K. P. O'Donnell, K. Lorenz, E. Alves, V. Matias, A. Vantomme, D. Wolverson, and I. M. Watson, J. Appl. Phys. **103**, 073510 (2008).
[45]I. Gorczyca, S. P. Lepkowski, T. Suki, N. E. Christensen, and A. Svane, Phys. Rev. B **80**, 075202 (2009).
[46]I. Gorczyca, T. Suski, N. E. Christensen, and A. Svane, Phys. Status Solidi C **7**, 1283 (2010).
[47]S. Schulz, M. A. Caro, L.-T. Tan, P. J. Parbrook, R. W. Martin, and E. P. O'Reilly, Appl. Phys. Express **6**, 121001 (2013).
[48]S. Schulz, M. A. Caro, and E. P. O'Reilly, Appl. Phys. Lett. **104**, 172102 (2014).
[49]V. Darakchieva, M. Beckers, M.-Y. Xie, L. Hultman, B. Monemar, J.-F. Carlin, E. Feltin, M. Gonschorek, and N. Grandjean, J. Appl. Phys. **103**, 103513 (2008).
[50]R. Butté, E. Feltin, J. Dorsaz, G. Christmann, J.-F. Carlin, N. Grandjean, and M. Ilegems, Jpn. J. Appl. Phys., Part 1 **44**, 7207 (2005).
[51]C. R. Abernathy, J. D. MacKenzie, S. R. Bharatan, K. S. Jones, and S. J. Pearton, J. Vac. Sci. Technol. A **13**, 716 (1995).
[52]T.-S. Yeh, J.-M. Wu, and W.-H. Lan, J. Crys. Growth **310**, 5308 (2008).
[53]G. Henkelman, B. P. Uberuga, and H. Jónsson, J. Chem. Phys. **113**, 9901 (2000).
[54]J. S. Blakemore, *Semiconductor statistics* (Pergamon, Oxford, 1962).
[55]G. Miceli and A. Pasquarello, Phys. Rev. B **93**, 165207 (2016).